

# Determining stress singularity exponents of plane V-notches in bonded bimaterial

NIU Zhong-rong<sup>1</sup>, GE Da-li<sup>1,2</sup>, CHENG Chang-zheng<sup>1</sup>, HU Zong-jun<sup>1</sup>

(1. School of Civil Engineering, Hefei University of Technology, Hefei 230009, China;  
2. School of Civil Engineering, Anhui Institute of Architecture, Hefei 230022, China)

**Abstract:** A new numerical method is proposed to determine the singularity orders of plane V-notch problems. Based on the assumption of asymptotic displacement field near the V-notch tip, the governing equations of the elastic theory were transformed into the eigenvalue problems of ordinary differential equations (ODEs) around the notch tip. Then the interpolating matrix method was further employed numerically to analyze the general eigenvalue problems of ODEs. Thus, the values of the singularity orders of the V-notches were determined through solving the corresponding ODEs by the interpolating matrix method. Two examples are given to illustrate the accuracy and effectiveness of the method.

**Key words:** stress singularity exponents; interpolating matrix method; V-notch

**CLC number:** O328      **Document code:** A

## 平面 V 形切口应力奇性指数分析

牛忠荣<sup>1</sup>, 葛大丽<sup>1,2</sup>, 程长征<sup>1</sup>, 胡宗军<sup>1</sup>

(1. 合肥工业大学土木建筑工程学院, 安徽合肥 230009; 2. 安徽建筑工业学院土木工程学院, 安徽合肥 230022)

**摘要:** 对于一般的 V 形切口结构, 其切口尖端区域存在强的应力集中. 基于切口尖端附近区域渐近应力场的假设, 提出将线弹性理论控制方程转换成一组常微分方程特征值问题. 然后采用插值矩阵法数值计算该常微分方程特征值问题, 从而得到 V 形切口的各阶应力奇性指数. 算例显示该方法是分析 V 形切口应力奇异指数的一个准确、有效的路径.

**关键词:** 应力奇异指数; 插值矩阵法; V 形切口

## 0 Introduction

The cases of V-notches of bonded dissimilar material are frequently encountered in engineering. There exists strong stress concentration near the

sharp notches and the interface ends. In particular, the peak stress at the notch tip is singular according to the elastic theory.

For a V-notch of homogeneous isotropic material with opening angle  $\alpha$ , as shown in Fig. 1,

**Received:** 2006-12-15; **Revised:** 2007-05-21

**Foundation item:** Supported by the Doctorial Program Foundation of the Ministry of Education (20050359009) and the Natural Science Foundation of Anhui Province (050440503).

**Biography:** NIU Zhong-rong (corresponding author), male, born in 1957, PhD/professor. E-mail: niu-zr@hfut.edu.cn

the singular stress field near the V-notch tip can be expressed as a series expansion with respect to the radial coordinate. One of the terms can be written as

$$\sigma_{ij} = A\rho^\lambda \tilde{\sigma}_{ij}(\theta) \quad (1)$$

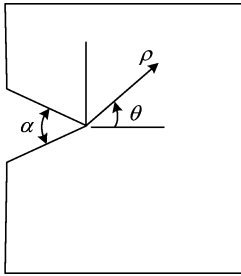


Fig. 1 A V-notch with opening angle  $\alpha$

where  $\lambda$  is called the singularity exponent/order. With the eigenfunction method, Williams<sup>[1]</sup> established the eigenequation as

$$\pm \lambda \sin \beta + \sin(\lambda\beta) = 0 \quad (2)$$

where  $\beta = 2\pi - \alpha$ . It can be seen that exponent  $\lambda$  depends on the notch angle  $\alpha$ .

In a general case of V-notch, the singularity exponents/orders may be either real or complex. Some methods have been proposed for treating various V-notch problems. Gross et al.<sup>[2]</sup> and Carpenter<sup>[3]</sup> obtained the stress intensity factors for plane V-notch problems by boundary collocation. Boundary element method was used to solve the displacement and stress field of plane V-notch problems<sup>[4, 5]</sup>. Through utilizing the solver of ordinary differential equation (ODE), Xu et al.<sup>[6]</sup> employed the inverse iteration method to search for the stress singularity orders of plane V-notch problems. However, it was only suitable to find the real roots among all solutions. With Eq. (2) as the starting point, the subregion accelerated Müller method<sup>[7]</sup> was utilized to compute the eigenvalues of the stress field near V-notch tip. Yao et al.<sup>[8]</sup> by using coherent gradient sensing (CGS) experimentally studied the stress singularity and fracture behaviors at mode-I V-notch tip. Recently, a special finite element method was used to deal with various V-notch problems based on the assumption of asymptotic

expansion of the stress field near V-notch tip. Chen et al.<sup>[9]</sup> proposed a new eigenanalysis method with hybrid finite element to determine the stress exponents and stress intensity factors of bonded bimaterial V-notches.

The aim of this paper is to analyze the stress singularities of plane V-notch problems of bonded bimaterial. The governing equations of linear elastic theory are transformed into the eigenvalue problems of ODEs based on the assumption of the asymptotic displacement field. Ref. [10] established the interpolating matrix method to solve two-point boundary value problems of ODEs. The method is further employed in the present work to solve the eigenvalue problems of ODEs.

## 1 The eigenvalue problems of ODEs for plane notches in linear elasticity

Firstly, let us consider a V-notch of isotropic material with opening angle  $2\pi - \theta_1 - \theta_2$  as shown in Fig. 2. Define a polar coordinate system  $\rho\theta$  in which the notch tip coincides with the pole. In terms of the linear elastic analysis, it has been verified that the asymptotic displacement field near the V-notch tip can be expressed in the following form

$$\left. \begin{aligned} u_\rho(\rho, \theta) &= \rho^{\lambda+1} \tilde{u}_\rho(\theta) \\ u_\theta(\rho, \theta) &= \rho^{\lambda+1} \tilde{u}_\theta(\theta) \end{aligned} \right\} \quad (3)$$

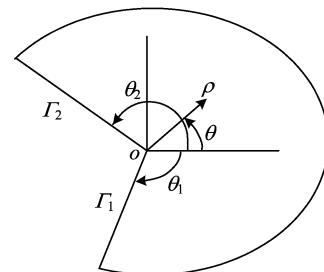


Fig. 2 Geometry of the notch

Introducing Eq. (3) into the geometrical equations of linear elastic theory yields the strain components as

$$\left. \begin{aligned} \varepsilon_\rho &= (1 + \lambda) \rho^\lambda \tilde{u}'_\rho(\theta) \\ \varepsilon_\theta &= \rho^\lambda \tilde{u}_\rho(\theta) + \rho^\lambda \tilde{u}'_\theta(\theta) \\ \gamma_{\rho\theta} &= \rho^\lambda \tilde{u}'_\rho(\theta) + \lambda \rho^\lambda \tilde{u}_\theta(\theta) \end{aligned} \right\} \quad (4)$$

where  $(\dots)' = d(\dots)/d\theta$ . In the case of plane stress, from Hooke's law the stresses are expressed as

$$\left. \begin{aligned} \sigma_\rho &= \frac{E}{1-\nu^2} \rho^\lambda [(1+\lambda)\tilde{u}_\rho + \nu\tilde{u}'_\rho + \tilde{u}'_\theta] \\ \sigma_\theta &= \frac{E}{1-\nu^2} \rho^\lambda [(1+\lambda)\nu\tilde{u}_\rho + \tilde{u}_\rho + \tilde{u}'_\theta] \\ \sigma_{\rho\theta} &= \frac{E}{2(1+\nu)} \rho^\lambda (\lambda\tilde{u}_\theta + \tilde{u}'_\rho) \end{aligned} \right\} \quad (5)$$

where  $E$  is the Young's modulus and  $\nu$  the Poisson ratio. Neglecting the body forces and substituting Eq. (5) into the equilibrium equations result in

$$\left. \begin{aligned} \tilde{u}''_\rho + \left(\frac{1+\nu}{1-\nu}\lambda - 2\right)\tilde{u}'_\rho + \frac{2}{1-\nu}\lambda(\lambda+2)\tilde{u}_\rho &= 0 \\ \tilde{u}''_\theta + \left[2 + \frac{1}{2}(1+\nu)\lambda\right]\tilde{u}'_\theta + \frac{1}{2}(1-\nu)\lambda(\lambda+2)\tilde{u}_\theta &= 0 \\ \theta \in (\theta_1, \theta_2) \end{aligned} \right\} \quad (6)$$

Assume that all of the tractions on the two edges  $\Gamma_1$  and  $\Gamma_2$  near the notch tip are zero. That is

$$\left. \begin{aligned} \left\{ \begin{matrix} \sigma_\theta \\ \sigma_{\rho\theta} \end{matrix} \right\}_{\theta=\theta_1} &= \left\{ \begin{matrix} \sigma_\theta \\ \sigma_{\rho\theta} \end{matrix} \right\}_{\theta=\theta_2} = \left\{ \begin{matrix} 0 \\ 0 \end{matrix} \right\} \end{aligned} \right\} \quad (7)$$

Hence, substitution of Eq. (5) into Eq. (7) yields

$$\left. \begin{aligned} \tilde{u}'_\theta + (1+\nu+\nu\lambda)\tilde{u}_\rho &= 0 \\ \tilde{u}'_\rho + \lambda\tilde{u}_\theta = 0, \theta = \theta_1 \text{ and } \theta_2 \end{aligned} \right\} \quad (8)$$

Observe that there is a factor  $\lambda^2$  in Eq. (6), which will lead to nonlinear eigenanalysis if Eq. (6) is solved directly. An alternative way for Eq. (6) is to introduce two new field variables as follows

$$\left. \begin{aligned} g_\rho(\theta) &= \lambda\tilde{u}_\rho(\theta), \theta \in (\theta_1, \theta_2) \\ g_\theta(\theta) &= \lambda\tilde{u}_\theta(\theta), \theta \in (\theta_1, \theta_2) \end{aligned} \right\} \quad (9)$$

Thus, utilizing Eq. (9), Eq. (6) can be rewritten as

$$\left. \begin{aligned} \tilde{u}''_\rho + \left(\frac{1+\nu}{1-\nu}\lambda - 2\right)\tilde{u}'_\rho + \frac{2}{1-\nu}(\lambda+2)g_\rho &= 0 \\ \tilde{u}''_\theta + \left[2 + \frac{1}{2}(1+\nu)\lambda\right]\tilde{u}'_\theta + \frac{1}{2}(1-\nu)(\lambda+2)g_\theta &= 0 \\ \theta \in (\theta_1, \theta_2) \end{aligned} \right\} \quad (10)$$

Summing up the above procedure, the evaluation of the singularity orders near the V-notch tip has been transformed into the linear eigenvalue problem of ODEs governed by Eqs. (9) and (10) subjected to the boundary condition of Eq. (8). Meanwhile, the corresponding eigenfunctions  $\tilde{u}_\rho$  and  $\tilde{u}_\theta$  can be achieved, which are useful to determine the stresses in the vicinity of the notch tip.

## 2 Evaluation of the stress singularity orders of the V-notches of bonded bimaterial

For the V-notch problem of bonded bimaterial, as shown in Fig. 3, the body consists of two subdomains of different materials.  $E_1$  and  $\nu_1$  are Yong's modulus and Poisson's ratio of the subdomain  $\Omega_1$ , respectively, while  $E_2$  and  $\nu_2$  are the ones of the subdomain  $\Omega_2$ . Observing the above derivation, it is known that Eqs. (9) and (10) are available for each subdomain for analyzing the stress singularity orders near the interface tip of the two materials. Thus, the governing equations are written as

$$\left. \begin{aligned} \tilde{u}''_{1\rho} + \left(\frac{1+\nu_1}{1-\nu_1}\lambda - 2\right)\tilde{u}'_{1\rho} + \frac{2}{1-\nu_1}(\lambda+2)g_{1\rho} &= 0 \\ \tilde{u}''_{1\theta} + \left[2 + \frac{1}{2}(1+\nu_1)\lambda\right]\tilde{u}'_{1\rho} + \frac{1}{2}(1-\nu_1)(\lambda+2)g_{1\theta} &= 0 \\ \theta \in (\theta_1, \theta_2) \end{aligned} \right\} \quad (11)$$

$$\left. \begin{aligned} g_{1\rho}(\theta) &= \lambda\tilde{u}_{1\rho}(\theta), \theta \in (\theta_1, \theta_2) \\ g_{1\theta}(\theta) &= \lambda\tilde{u}_{1\theta}(\theta), \theta \in (\theta_1, \theta_2) \end{aligned} \right\} \quad (12)$$

and

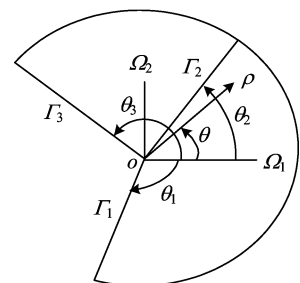


Fig. 3 A V-notch of bonded bimaterial

$$\left. \begin{aligned} &\tilde{u}''_{2\rho} + \left(\frac{1+\nu_2}{1-\nu_2}\lambda - 2\right)\tilde{u}'_{2\rho} + \frac{2}{1-\nu_2}(\lambda+2)g_{2\rho} = 0 \\ &\tilde{u}''_{2\theta} + \left[2 + \frac{1}{2}(1+\nu_2)\lambda\right]\tilde{u}'_{2\rho} + \\ &\frac{1}{2}(1-\nu_2)(\lambda+2)g_{2\theta} = 0, \quad \theta \in (\theta_2, \theta_3) \end{aligned} \right\} \quad (13)$$

$$\left. \begin{aligned} &g_{2\rho}(\theta) = \lambda\tilde{u}_{2\rho}(\theta), \quad \theta \in (\theta_2, \theta_3) \\ &g_{2\theta}(\theta) = \lambda\tilde{u}_{2\theta}(\theta), \quad \theta \in (\theta_2, \theta_3) \end{aligned} \right\} \quad (14)$$

where  $\tilde{u}_{1\rho}(\theta)$ ,  $\tilde{u}_{1\theta}(\theta)$  are the eigenfunctions of displacement components in subdomain  $\Omega_1$  near the notch tip,  $\tilde{u}_{2\rho}(\theta)$ ,  $\tilde{u}_{2\theta}(\theta)$  are ones in subdomain  $\Omega_2$ . For the bonded bimaterial, the displacement components and the interface tractions are compatible on  $\Gamma_2$ . This means

$$\left. \begin{aligned} &\tilde{u}_{1\rho}(\theta_2) = \tilde{u}_{2\rho}(\theta_2) \\ &\tilde{u}_{1\theta}(\theta_2) = \tilde{u}_{2\theta}(\theta_2) \end{aligned} \right\} \quad (15)$$

$$\left. \begin{aligned} &\left\{ \begin{matrix} \sigma_{1\theta} \\ \sigma_{1\rho\theta} \end{matrix} \right\}_{\theta=\theta_2} = \left\{ \begin{matrix} \sigma_{2\theta} \\ \sigma_{2\rho\theta} \end{matrix} \right\}_{\theta=\theta_2} \end{aligned} \right\} \quad (16)$$

Substitution of Eq. (5) into Eq. (16) gives

$$\left. \begin{aligned} &\frac{E_1}{1-\nu_1^2}[\tilde{u}'_{1\theta} + (1+\nu_1+\nu_1\lambda)\tilde{u}_{1\rho}] - \\ &\frac{E_2}{1-\nu_2^2}[\tilde{u}'_{2\theta} + (1+\nu_2+\nu_2\lambda)\tilde{u}_{2\rho}] = 0 \\ &\frac{E_1}{2(1+\nu_1)}(\tilde{u}'_{1\rho} + \lambda\tilde{u}_{1\theta}) - \\ &\frac{E_2}{2(1+\nu_2)}(\tilde{u}'_{2\rho} + \lambda\tilde{u}_{2\theta}) = 0, \quad \theta = \theta_2 \end{aligned} \right\} \quad (17)$$

Similar to Eq. (8), the boundary conditions on  $\Gamma_1$  and  $\Gamma_3$  are traction-free as

$$\left. \begin{aligned} &\tilde{u}'_{1\theta} + (1+\nu_1+\nu_1\lambda)\tilde{u}_{1\rho} = 0, \quad \theta = \theta_1 \\ &\tilde{u}'_{1\rho} + \lambda\tilde{u}_{1\theta} = 0, \quad \theta = \theta_1 \end{aligned} \right\} \quad (18)$$

$$\left. \begin{aligned} &\tilde{u}'_{2\theta} + (1+\nu_2+\nu_2\lambda)\tilde{u}_{2\rho} = 0, \quad \theta = \theta_3 \\ &\tilde{u}'_{2\rho} + \lambda\tilde{u}_{2\theta} = 0, \quad \theta = \theta_3 \end{aligned} \right\} \quad (19)$$

Therefore, the evaluation of the singularity orders  $\lambda$  near the V-notch tip of bonded bimaterial has been transformed into solving ODEs Eqs. (11)~(14) and boundary conditions Eqs. (15), (17)~(19).

There have been some numerical ways to find the solution of the ODEs. At present, the most commonly used methods for solving ODEs are the finite difference, shooting and collocation

methods. Ref. [10] established a numerical method by the name of interpolating matrix method to solve BVPs in ODEs, which chooses the highest derivative in the ODEs as the unknowns of the discrete system of the ODEs. Here the interpolating matrix method is further employed as a solver of the eigenvalue problems of ODEs. Consequently, the stress singularity orders are obtained by implementing the interpolating matrix method for the ODEs of the V-notches.

### 3 Numerical examples

**Example 3.1** A V-notch of isotropic material as shown in Fig. 2.

With the subregion accelerated Müller method, Fu et al. [7] computed a number of the eigenvalues of the stress singularity orders of the V-notch problem. Here the interpolating matrix method (IMM) is used to solve the ODEs Eqs. (10), (9) and (8) where  $\nu=0.3$ . The results are given in Tabs. 1 and 2, in which  $\alpha$  is the opening angle. The eigenvalues  $\lambda$  are often complexes expressed by  $\lambda_k = \xi_k + i\eta_k$  where  $i = \sqrt{-1}$ . Tab. 1 lists the eigenvalues corresponding to the symmetrical displacement (mode I) eigenfunction  $\tilde{u}_\rho(\theta)$  and Tab. 2 lists the ones corresponding to the anti-symmetrical displacement (mode II) eigenfunction  $\tilde{u}_\theta(\theta)$ , where  $n$  is the number of the divisions within interval  $[\theta_1, \theta_2]$  in IMM.

Tabs. 1 and 2 show that the eigenvalues obtained by using IMM are in good agreement with the results of Ref. [7] as  $n$  increases. Note that the eigenvalues whose real parts are between  $-1$  and  $0$ , i. e.  $\text{Re}(\lambda) \in (-1, 0)$  should be paid more attention to, which indicates that the stress field at the V-notch tip is singular. It is found that there exist either one or two real eigenvalues in the range of  $-0.5 \leq \lambda_k < 0$  when  $0 \leq \alpha \leq 180^\circ$  for the V-notch of isotropic material. All the first two eigenvalues for the schemes of  $n=40$  in Tabs. 1 and 2 have converged up to the fourth significant figure.

**Tab. 1 The eigenvalues corresponding to the symmetrical displacement eigenfunction  $\tilde{u}_\rho(\theta)$**

$\alpha$	methods	$\xi_1$	$\eta_1$	$\xi_2$	$\eta_2$	$\xi_3$	$\eta_3$	$\xi_4$	$\eta_4$
170°	Ref. [7]	-0.099 956	0	1.001 795	0	1.695 232	0	3.022 680	0
	IMM, $n=20$	-0.099 767 1	0	1.000 629	0	1.706 359	0	2.972 986	0
	IMM, $n=40$	-0.099 949	0	1.001 733	0	1.695 693	0	3.020 562	0
150°	Ref. [7]	-0.248 025	0	1.106 286	0.096 100	2.828 294	0.347 177	4.547 288	0.459 268
	IMM, $n=20$	-0.247 871	0	1.109 776	0.087 307	2.859 206	0.321 400	4.705 928	0.308 320
	IMM, $n=40$	-0.248 019	0	1.106 531	0.095 588	2.830 449	0.345 590	4.556 639	0.452 879
120°	Ref. [7]	-0.384 269	0	0.833 549	0.252 251	2.343 717	0.414 037	3.849 458	0.506 015
	IMM, $n=20$	-0.384 138	0	0.836 062	0.252 153	2.365 450	0.414 282	3.957 761	0.498 516
	IMM, $n=40$	-0.384 259	0	0.833 734	0.252 249	2.345 190	0.414 126	3.856 164	0.506 382
90°	Ref. [7]	-0.455 516	0	0.629 257	0.231 251	1.971 844	0.373 931	3.310 377	0.455 494
	IMM, $n=20$	-0.455 395	0	0.631 172	0.232 519	1.988 336	0.383 516	3.394 304	0.488 602
	IMM, $n=40$	-0.455 511	0	0.629 323	0.231 332	1.972 392	0.374 414	3.313 047	0.457 263
60°	Ref. [7]	-0.487 779	0	0.471 028	0.141 853	1.677 615	0.284 901	2.881 487	0.360 496
	IMM, $n=20$	-0.487 717	0	0.471 813	0.143 640	1.684 805	0.296 623	2.924 016	0.408 020
	IMM, $n=40$	-0.487 775	0	0.471 073	0.141 991	1.678 017	0.285 650	2.883 292	0.363 632
30°	Ref. [7]	-0.498 547	0	0.202 957	0	0.490 378	0	1.440 492	0.114 207
	IMM, $n=20$	-0.498 472	0	0.205 806	0	0.488 633	0	1.445 210	0.147 248
	IMM, $n=40$	-0.498 540	0	0.203 164	0	0.490 268	0	1.440 740	0.116 222
10°	Ref. [7]	-0.499 947	0	0.058 843	0	0.499 728	0	1.118 823	0
	IMM, $n=20$	-0.499 856	0	0.060 933	0	0.498 345	0	1.151 176	0
	IMM, $n=40$	-0.499 934	0	0.059 126	0	0.499 521	0	1.122 380	0
0°	Exact solu.	-0.500 00	0	0	0	0.500 00	0	1.000 00	0
	IMM, $n=20$	-0.499 794	0	0.003 578	0	0.497 325	0	1.043 82	0
	IMM, $n=40$	-0.499 985	0	0.000 257	0	0.499 804	0	1.002 93	0

**Tab. 2 The eigenvalues corresponding to the anti-symmetrical displacement eigenfunction  $\tilde{u}_\rho(\theta)$**

$\alpha$	methods	$\xi_1$	$\eta_1$	$\xi_2$	$\eta_2$	$\xi_3$	$\eta_3$	$\xi_4$	$\eta_4$	$\xi_5$	$\eta_5$
170°	Ref. [7]	0.798 933	0	0	0	2.007 826	0	2.586 721	0	4.060 480	0
	IMM, $n=20$	0.800 916	0	0	0	1.997 193	0	2.631 530	0	3.902 388	0
	IMM, $n=40$	0.799 004	0	0	0	2.007 389	0	2.588 412	0	4.048 878	0
150°	Ref. [7]	0.485 814	0	0	0	1.967 836	0.261 186	3.688 038	0.409 575	5.406 179	0.500 793
	IMM, $n=20$	0.487 279	0	0	0	1.979 418	0.249 763	3.760 510	0.349 527	5.467 941	0
	IMM, $n=40$	0.485 919	0	0	0	1.968 624	0.260 421	3.692 685	0.406 489	5.422 865	0.490 318
120°	Ref. [7]	0.148 913	0	0	0	1.589 479	0.348 375	3.090 928	0.464 641	4.601 514	0.541 087
	IMM, $n=20$	0.150 009	0	0	0	1.597 549	0.348 528	3.147 310	0.463 943	4.820 487	0.503 578
	IMM, $n=40$	0.148 992	0	0	0	1.590 100	0.348 397	3.100 330	0.464 789	4.614 583	0.541 504
90°	Ref. [7]	-0.091 471	0	0	0	1.301 327	0.315 838	2.641 420	0.418 787	3.978 902	0.486 625
	IMM, $n=20$	-0.090 574	0	0	0	1.307 470	0.319 829	2.680 315	0.437 987	4.148 389	0.532 426
	IMM, $n=40$	-0.091 436	0	0	0	1.301 562	0.315 956	2.642 884	0.419 538	3.984 719	0.489 385
60°	Ref. [7]	-0.269 099	0	0	0	1.074 826	0.229 426	2.279 767	0.326 690	3.482 900	0.388 984
	IMM, $n=20$	-0.268 710	0	0	0	1.077 382	0.234 207	2.297 998	0.351 998	3.574 251	0.469 510
	IMM, $n=40$	-0.269 070	0	0	0	1.075 014	0.229 741	2.280 884	0.328 306	3.487 289	0.394 444
30°	Ref. [7]	-0.401 808	0	0	0	0.838 934	0	0.948 560	0	1.987 005	0.166 741
	IMM, $n=20$	-0.401 460	0	0	0	0.881 197	0	0.909 578	0	1.999 550	0.222 443
	IMM, $n=40$	-0.401 781	0	0	0	0.840 591	0	0.947 180	0	1.987 897	0.170 364
10°	Ref. [7]	-0.470 645	0	0	0	0.588 609	0	0.999 107	0	1.649 700	0
	IMM, $n=20$	-0.470 319	0	0	0	0.597 760	0	0.991 337	0	1.770 116	0
	IMM, $n=40$	-0.470 599	0	0	0	0.589 736	0	0.998 226	0	1.659 348	0
0°	Exact solu.	-0.500 00	0	0	0	0.500 000	0	1.000 000	0	1.500 00	0
	IMM, $n=20$	-0.499 373	0	0	0	0.513 993	0	0.987 129	0	1.625 22	0
	IMM, $n=40$	-0.499 954	0	0	0	0.500 983	0	0.999 039	0	1.507 41	0

**Tab. 3** The eigenvalues of the V-notch with  $\theta_1 = 0^\circ$ ,  $\theta_2 = 135^\circ$ ,  $\theta_3 = 270^\circ$ ,  $\nu_1 = \nu_2 = 0.3$ 

Ref. [11]	Interpolating matrix method							
	$n=20$		$n=40$		$n=80$			
$E_1/E_2$	$\lambda_1$	$\lambda_2$	$\lambda_1$	$\lambda_2$	$\lambda_1$	$\lambda_2$	$\lambda_1$	$\lambda_2$
1	-0.455 52	-0.091 47	-0.455 504 8	-0.091 462 3	-0.455 515 7	-0.091 466 6	-0.455 516 2	-0.091 470 4
3	-0.434 60	-0.127 80	-0.434 562 4	-0.127 775 7	-0.434 596 1	-0.127 796 9	-0.434 596 5	-0.127 800 3
5	-0.413 94	-0.160 25	-0.414 128 9	-0.159 984 7	-0.413 938 0	-0.160 247 5	-0.413 938 4	-0.160 250 7
7	-0.398 22	-0.183 06	-0.398 202 2	-0.183 117 2	-0.398 218 9	-0.183 058 2	-0.398 219 2	-0.183 061 4
10	-0.380 32	-0.207 35	-0.380 319 2	-0.207 299 9	-0.380 319 9	-0.207 342 2	-0.380 320 1	-0.207 345 3

**Example 3.2** A V-notch of bonded dissimilar bimaterial as shown in Fig. 3.

The V-notch is considered as the plane stress problem. The bonded interface lies at  $\theta = \theta_2$ . The Poisson's ratios of the materials are  $\nu_1 = \nu_2 = 0.3$ , and  $E_2/E_1$  is variable. In Ref. [11], Newton's iteration is used to calculate the stress singularities through an eigenequation derived by means of complex functions. In the case of the bimaterial V-notch, there exist two real eigenvalues in the range of  $-1 < \lambda_k < 0$ . In applying IMM, the two intervals  $[\theta_1, \theta_2]$  and  $[\theta_2, \theta_3]$  are divided into the same number of subintervals, where  $n$  denotes the number of the divisions within each interval.  $\lambda_1$  and  $\lambda_2$  obtained by using IMM are shown in Tab. 3 for given  $\theta_1 = 0^\circ$ ,  $\theta_2 = 135^\circ$ ,  $\theta_3 = 270^\circ$ . It can be seen in Tab. 3 that the present solutions converge and agree well with the results of Ref. [11]. In fact, apart from the very small imaginary components, all the first six  $\lambda_k = \xi_k + i\eta_k$ , ( $k=1, \dots, 6$ ), obtained by using IMM with  $n=40$  are converged up to the fourth significant figure.

## 4 Conclusions

For determining the singularity orders at the plane V-notch tips, the governing differential equations of linear elastic theory are transformed into the eigenvalue problem of ODEs based on the assumption of the asymptotic displacement field. Then IMM is employed numerically to analyze the eigenvalue problems of ODEs. As an application, the values of the main singularity orders of plane V-notch problems are achieved through solving the ODEs from the notches. Finally, two examples are given to show the application of the present

method for determining the singularity orders of the plane V-notches.

## References

- [1] Williams M L. Stress singularities resulting from various boundary conditions in angular corners of plates in tension [J]. Journal of Applied Mechanics, 1952, 19: 526-534.
- [2] Gross B, Srawley J E, Brown W F. Stress intensity factors for a single-edge-notch tension specimen by boundary collocation[R]. NASA Technical Note D-2395, 1964.
- [3] Carpenter W C. The eigenvector solution for a general corner or finite opening crack with further studies on the collocation procedure[J]. International Journal of Fracture, 1985, 27(1): 63-73.
- [4] Rzasnicki W, Mendelson A, Albers L U. Application of boundary integral method to elastoplastic analysis of V-notched beams [J]. International Journal of Fracture, 1975, 11: 329-342.
- [5] Tan C L, Gao Y L, Afagh F F. Boundary element analysis of interface cracks between dissimilar anisotropic materials[J]. International Journal of Solids and Structures, 1992, 29(24): 3 201-3 220.
- [6] Xu Y J, Yuan S. Complete eigen-solution for anti-plane notches with multi-materials by super-inverse iteration[J]. ACTA Mechanica Sinica, 1997, 10(2): 157-166.
- [7] 傅向荣, 龙驭球. 解析试函数法分析平面切口问题 [J]. 工程力学, 2003, 20(4): 33-38, 73.
- [8] Yao X F, Yeh H Y, Xu W. Fracture investigation at V-notch tip using coherent gradient sensing (CGS)[J]. International Journal of Solid and Structure, 2006, 43 (5): 1 189-1 200.
- [9] Chen M C, Sze K Y. A novel finite element analysis of bimaterial wedge problems[J]. Engineering Fracture Mechanics, 2001, 68(13): 1 463-1 476.
- [10] Niu Z R. Nonlinear bending of the shallow spherical shells with variable thickness under axisymmetrical loads[J]. Applied Mathematics and Mechanics, 1993, 14(11): 1 023-1 031.
- [11] 简政, 黄松海, 胡黎明. 双材料 V 形切口应力强度因子计算及其在重力坝中的应用[J]. 水利学报, 1998, (6): 77-81.